

Massive Free-Streaming Neutrinos and Rise of N_ν at Recombination

Jeremiah Birrell¹, Cheng-Tao Yang^{2,3}, Pisin Chen^{2,3,4}, and Johann Rafelski⁵

¹*Program in Applied Mathematics,
The University of Arizona,
Tucson, Arizona, 85721, USA*

²*Department of Physics and Graduate Institute of Astrophysics,
National Taiwan University, Taipei, Taiwan 10617*

³*Leung Center for Cosmology and Particle Astrophysics (LeCosPA),
National Taiwan University, Taipei, Taiwan, 10617*

⁴*Kavli Institute for Particle Astrophysics and Cosmology,
SLAC National Accelerator Laboratory,
Menlo Park, CA 94025, USA and*

⁵*Department of Physics, The University of Arizona,
Tucson, Arizona, 85721, USA
(Dated: December 30, 2012)*

We present the Einstein-Vlasov solution for the momentum distribution of the relic free-streaming neutrinos. We show that it is possible to explain the rise in the effective number of neutrinos N_ν from those present at the end of the big bang nucleosynthesis (BBN) $N_\nu(T_{BBN}) = 3.71^{+0.47}_{-0.45}$ towards $N_\nu(T_r) = 4.34^{+0.086}_{-0.88}$ noted at time of electron-ion recombination (r). This increase is due to the interplay of the neutrino mass and the non-equilibrium form of the neutrino distribution after the freeze-out. One implication of our scenario is that the mass of the heaviest neutrino should be near the recombination temperature, $T_r = 0.253$ eV. If instead of the Einstein-Vlasov solution, a thermal equilibrium distribution is inadvertently invoked, one would expect a decrease in N_ν at recombination.

PACS numbers: 51.10.+y, 95.30.Cq, 14.60.Pq, 26.35.+c

I. INTRODUCTION

The relic (i.e. background cosmic) neutrinos have not been directly measured [1, 2]. Their presence and properties are inferred from reaction dynamics throughout the history of the universe [3, 4]. Chemical freeze-out occurs when particle number changing reactions stop due to the expansion of the Universe and a decrease in particle densities near $T_{ch} \simeq 3.3$ MeV. All 2-into-2 particle collisions involving neutrinos cease near $T_f \simeq 2.3$ MeV and neutrinos begin to free-stream, akin to the free-streaming of photons after atoms form and ion-electron plasma entirely disappears at the much lower recombination temperature $T_r = 0.253 \pm 0.001$ eV [5, 6]. In a future work we will present a detailed study of the different chemical and kinetic freeze-out neutrino conditions [7].

After neutrino abundance i.e. chemical equilibrium condition is reached (chemical freeze-out) there are some known processes that feed into the neutrino gas and result in a post-equilibrium addition to the

neutrino abundance, an effect that has been studied extensively in the literature [8]. To quantify this effect one introduces effective number abundance of neutrinos of N_ν defined as the relic neutrino to the photon energy density ratio, allowing for photon to massless fermion statistical ratio 7/8, to be compared to the standard model which contains exactly $N_\nu = 3$ left handed neutrino flavors.

The modification due to two body reactions involving neutrinos and e^\pm from neutrino chemical (abundance) freeze-out until the time when positrons have annihilated was calculated in [9] and we will often refer to this value $N_\nu^{\text{th}}(T_{BBN}) \equiv N_\nu^{\text{thBBN}} = 3.046$. Neutrino feeding occurs in the BBN phase finishing at $T_{BBN} \simeq m_e/10$ but the net result is smaller [10]. All three flavors are strongly mixing as a function of time. In the early universe environment as long as at least one of the neutrinos remains in equilibrium with the background, all three flavors participate in the kinetic processes equilibrating with the background, consisting mainly of photons and electron-positron

plasma.

There is currently a significant degree of interest in the precise value of N_ν . Studies of the cosmic microwave background (CMB) and element production during big bang nucleosynthesis (BBN) put constraints on the effective number of neutrinos. In the WMAP 7-year report [11] the effective number of neutrinos at recombination $T_r = 0.253$ eV is $N_\nu(T_r) \equiv N_\nu^r = 4.34^{+0.086}_{-0.88}$, while the current value deduced from BBN is $N_\nu(T_{BBN}) \equiv N_\nu^{BBN} = 3.71^{+0.47}_{-0.45}$ [4, 12]. The errors inherent in the analyzed data are large and so it is certainly possible that the measurements by these different methods agree, and agree with the theoretical result $N_\nu^{\text{th}}(T_{BBN})$.

On the other hand these results indicate that there is an increase in $N_\nu(T)$ between the end of the BBN epoch and recombination. We will show that one would naturally expect an increase in N_ν when the effective neutrino temperature approaches the neutrino mass. To obtain this result we employ that fact that once kinetic (commonly called thermal) freeze-out has occurred, neutrinos in essence free-stream (up to additional e.g. e^+e^- annihilation-feeding [9]). We must therefore use solutions of the Boltzmann-Einstein-Vlasov (commonly called Einstein-Vlasov) non-equilibrium kinetic evolution equation to describe how the neutrino momentum distribution changes in an expanding universe after kinetic freeze-out. Such solutions will preserve the comoving entropy and neutrino particle number, which a Fermi-Dirac integrated equilibrium distribution in general does not do.

Interestingly, an increase in N_ν constitutes an independent measurement of the mass of neutrino(s) near to the recombination epoch, which has gone unnoticed. The essential physics ingredients for neutrino mass to make a mark are

1. At least one neutrino has a mass near the value of the temperature when the universe becomes transparent to photons at $T_r = 0.253$ eV e.g. where neutrino density becomes a part of WMAP acoustical oscillation analysis [11];
2. After kinetic freeze-out, but in particular near to the T_r -epoch, neutrinos free stream through an expanding universe. Their momentum distribution is thus not in equilibrium. It will be seen that the thermal momentum shape can only persist when the free-streaming particle is massless, as is the case for photons.
3. The effective neutrino number at any epoch where they are already free-stream, e.g. at BBN, is known. This allows one to fix the

magnitude of enhancement factor. Deviation from $N_\nu = 3$ at BBN is not necessary, but it affects the predicted value of the neutrino mass.

We stress that the nonzero mass of the neutrino combined with the non-equilibrium form of the free-streaming distribution offers a novel mechanism for increasing the value of N_ν .

In section II we discuss the non-equilibrium properties of neutrinos. In subsection II A we derive the form of the neutrino distribution using the Einstein-Vlasov equation. In subsection II B we compute various moments of the distribution. In subsection II C we compute the photon reheating temperature. In section III we combine our results and demonstrate that the effective number of neutrinos rises between BBN and ion-electron recombination. In subsection III A we describe the change in the effective number of neutrinos while in subsection III B we show that if one incorrectly assumes a kinetic (thermal) equilibrium Fermi neutrino distribution, one finds that N_ν decreases. We present our conclusions and discussion in section IV.

II. NONEQUILIBRIUM NEUTRINOS

A. Einstein-Vlasov Equation in FRW Spacetime

Prior to the neutrino freeze-out temperature, $T_f \simeq 2.3$ MeV, collisions are significant and keep neutrinos in kinetic (thermal) equilibrium, implying that the distribution function of each neutrino flavor has the Fermi-Dirac form

$$f_{\text{FD}}(t, E) = \frac{g_\nu}{8\pi^3} [\exp(E/T) + 1]^{-1} \text{ for } T \geq T_f \quad (1)$$

where $g_\nu = 2$ is the degeneracy of each neutrino flavor. When the temperature drops below T_f , interactions no longer occur rapidly enough to keep the distribution in thermal equilibrium and the neutrinos begin to freely stream. The neutrinos are no longer in equilibrium, and hence kinetic theory must be utilized to describe the evolution of their distribution function.

The general relativistic Boltzmann equation describes the dynamics of a gas of particles that travel freely in between point interactions in an arbitrary spacetime [13–16]

$$p^\alpha \partial_{x^\alpha} f - \Gamma_{\mu\nu}^j p^\mu p^\nu \partial_{p_j} f = C[f]. \quad (2)$$

Here $\Gamma_{\mu\nu}^\alpha$ is the affine connection (Christoffel symbol), f is a function on the mass shell

$$g_{\alpha\beta}p^\alpha p^\beta = m^2, \quad (3)$$

hence Greek indices are summed from 0 to 3 whereas j is only summed from 1 to 3. When collisions are negligible $C[f] = 0$ and all particles move on geodesics, yielding the Einstein-Vlasov equation.

We now specialize to collision free homogeneous isotropic cosmological solutions and therefore assume the flat FRW ansatz for the spacetime metric

$$g = dt^2 - a(t)^2(dx^2 + dy^2 + dz^2). \quad (4)$$

Due to homogeneity and isotropy, the distribution function depends on t and $p^0 = E$ only. Therefore Eq. (2) becomes

$$E\partial_t f + (m^2 - E^2)\frac{\partial_t a}{a}\partial_E f = 0. \quad (5)$$

The general solution to Eq. (5) is known [15]:

$$f(t, E) = K(x), \quad x = \frac{a(t)^2}{D^2}(E^2 - m^2), \quad (6)$$

where K is an arbitrary smooth function and D is an arbitrary constant with units of mass. To continue the evolution beyond the freeze out time, t_f , we must choose K to match at t_f the equilibrium distribution Eq. (1).

As mentioned in the introduction, after chemical freeze-out there are additional processes that can feed into the neutrino distribution. To account for this we include a fugacity factor, Υ , that allows for a possible overabundance of neutrinos. The effect of $\Upsilon = e^\sigma$ is modeled after that of chemical potential μ , except that σ is equal for particles and antiparticles, and not opposite. This means $\sigma > 0$ ($\Upsilon > 1$) increases the density of both particles and antiparticles, rather than increasing one and decreasing the other as is common when the chemical potential is associated with conservation laws such as lepton number. The fact that σ is not opposite for particles and antiparticles reflects the fact that both the number of particles and the number of antiparticles are conserved after chemical freeze-out, and not just their difference. The equality reflects the fact that any process that modifies the distribution would affect both particle and antiparticle distributions in the same fashion.

The use of Υ to account for the processes that feed into neutrinos is exact in the temperature interval after chemical and before kinetic freeze-out, since scattering processes re-equilibrate the momentum distribution to this shape in order to maximize

the entropy content. However, it is an approximation when the additional particle feeding occurs below kinetic freeze-out: when using the Υ -modeled distribution, we are making an assumption about how such feeding affects the momentum distribution. The computed effect of e^+e^- annihilation-feeding [9] is small, below 5%, so the potential error of this assumption is not significant.

With this in mind, we let

$$K(x) = \frac{g_\nu}{8\pi^3} \frac{1}{\Upsilon^{-1} e^{\sqrt{x+m^2/T_f^2}} + 1} \quad (7)$$

and $D = T_f a(t_f)$ to match the Fermi-Dirac (FD) distribution at freeze-out. The Fermi-Dirac-Einstein-Vlasov (FDEV) distribution function after freeze-out is then

$$f(t, E) = \frac{g_\nu}{8\pi^3} \frac{1}{\Upsilon^{-1} e^{\sqrt{(E^2-m^2)/T_\nu^2 + m^2/T_f^2}} + 1} \quad (8)$$

where

$$T_\nu(t) = \frac{T_f a(t_f)}{a(t)}. \quad (9)$$

Eq. (8) provides the distribution function that describes a gas of neutrinos that have been free streaming in an expanding universe since they froze out at $T_\nu(t_f) = T_f$, with a possible overabundance represented by the fugacity Υ . We will call T_ν in Eq. (9) the neutrino background temperature, even though the distribution of free streaming particles has a thermal shape only for $m = 0$. This language is, however, reasonable since apart from the reheating factor of photons due to e^+e^- annihilation, which we discuss in subsection II C, T_ν is equal to the photon background temperature.

B. Moments of the FDEV Distribution

Here we compute the stress energy tensor, number current, and entropy current associated with the distribution Eq. (8)

$$\mathcal{T}^{\mu\nu} = \int f \frac{p^\mu p^\nu}{p_0} \sqrt{-g} d^3 p, \quad (10)$$

$$n^\nu = \int f \frac{p^\nu}{p_0} \sqrt{-g} d^3 p, \quad (11)$$

$$s^\mu = -\frac{g_\nu}{8\pi^3} \int h \frac{p^\mu}{p_0} \sqrt{-g} d^3 p, \quad (12)$$

$$h = \tilde{f} \ln(\tilde{f}) + (1 - \tilde{f}) \ln(1 - \tilde{f}), \quad \tilde{f} = \frac{8\pi^3}{g_\nu} f.$$

We first work with the general form of f given in Eq. (6) and later specialize to the explicit form Eq. (8).

Isotropy of the metric and of f in momentum space implies that the off diagonal elements of the stress energy tensor and spacial components of the particle number and entropy currents vanish and that the pressure is isotropic. Hence we must compute

$$\mathcal{T}^{00} = a^3 \int f E d^3 p, \quad (13)$$

$$\mathcal{T}^{ii} = \frac{1}{3} a^3 \int f \frac{|p|^2}{E} d^3 p, \quad i = 1 \dots 3, \quad (14)$$

$$n^0 = a^3 \int f d^3 p, \quad (15)$$

$$s^0 = -a^3 \frac{g_\nu}{8\pi^3} \int h d^3 p \quad (16)$$

where $|p|$ is the Euclidean norm of the spacial components of p^μ and $E = p^0$ is given by

$$m^2 = E^2 - a(t)^2 |p|^2. \quad (17)$$

Computing \mathcal{T}^{00} we find

$$\begin{aligned} \mathcal{T}^{00} &= 4\pi a^3 \int_0^\infty K((E^2 - m^2)/T_\nu^2) E |p|^2 d|p| \\ &= 4\pi a^3 \int_0^\infty K(a^2 p^2/T_\nu^2) (m^2 + a^2 p^2)^{1/2} |p|^2 d|p| \\ &= 4\pi \int_0^\infty K(z^2/T_\nu^2) (m^2 + z^2)^{1/2} z^2 dz \end{aligned} \quad (18)$$

where we made a change of variables $z = a(t)|p|$. Note that z is the physically measured momentum. Similarly

$$\mathcal{T}^{ii} = \frac{4\pi}{3a^2} \int_0^\infty K(z^2/T_\nu^2) (m^2 + z^2)^{-1/2} z^4 dz, \quad (19)$$

$$n^0 = 4\pi \int_0^\infty K(z^2/T_\nu^2) z^2 dz, \quad (20)$$

$$s^0 = -\frac{g_\nu}{2\pi^2} \int_0^\infty H(z^2/T_\nu^2) z^2 dz, \quad (21)$$

$$H = \tilde{K} \ln \tilde{K} + (1 - \tilde{K}) \ln(1 - \tilde{K}), \quad \tilde{K} = \frac{8\pi^3}{g_\nu} K. \quad (22)$$

We now rename z to p , so that p represents the magnitude of the physical momentum, drop the superscripts, and insert Eq. (7) for K , giving the energy density, pressure, and number density for each

neutrino flavor

$$\rho = \frac{g_\nu}{2\pi^2} \int_0^\infty \frac{(m^2 + p^2)^{1/2} p^2 dp}{\Upsilon^{-1} e^{\sqrt{p^2 + m^2}(T_\nu^2/T_f^2)/T_\nu} + 1}, \quad (23)$$

$$P = \frac{g_\nu}{6\pi^2} \int_0^\infty \frac{(m^2 + p^2)^{-1/2} p^4 dp}{\Upsilon^{-1} e^{\sqrt{p^2 + m^2}(T_\nu^2/T_f^2)/T_\nu} + 1}, \quad (24)$$

$$n = \frac{g_\nu}{2\pi^2} \int_0^\infty \frac{p^2 dp}{\Upsilon^{-1} e^{\sqrt{p^2 + m^2}(T_\nu^2/T_f^2)/T_\nu} + 1}. \quad (25)$$

These differ from the corresponding expressions for an equilibrium distribution in Minkowski space by the $T_\nu(t)/T_f$ factor multiplying m *only* in the exponential.

By making a change of variables $u = p/T_\nu$, one sees that both n and s are proportional to T_ν^3 . By definition, T_ν is inversely proportional to a , hence

$$a^3 n = \text{constant and } a^3 s = \text{constant}. \quad (26)$$

This proves that the particle number and entropy in a comoving volume are conserved. This result does not depend on the particular form of K chosen above. Note further that since an eV scale or below neutrino mass is at least 6 orders of magnitude smaller than T_f , we can ignore the neutrino mass in the exponent. This remark does not extend to the energy factor multiplying the FD-distribution in the calculation of energy density or pressure and therefore Eq. (23) and Eq. (24) have unusual properties, while Eq. (25) is just what one may naively expect, remembering that the mass term in this expression is completely negligible.

C. Photon and neutrino temperatures

To compare our results with observation, we must understand the photon to neutrino temperature ratio. The difference between the two is the result of the annihilation of e^+e^- , mainly into photons. Before this reheating, neutrinos, photons, electrons, and positrons have the same temperature. When the temperature approaches and drops below the electron mass, the electrons and positrons annihilate. The resulting ratio of photon to neutrino temperatures has often been studied but not in the type of non-equilibrium model presented here. After photon reheating, both the neutrino and photon temperatures evolve inversely proportional to a , so their ratio after reheating equals their ratio today. We use subscripts 1 and 2 to denote quantities before and after reheating, respectively.

Before reheating, the entropy in a given volume, V_1 , is the sum of relativistic neutrinos, electrons, positrons, and photons

$$S_1 = \left(3\frac{7}{8}g_\nu + \frac{7}{8}g_{e^\pm} + g_\gamma \right) \frac{2\pi^2}{45} T_1^3 V_1 \quad (27)$$

where T_1 is the common neutrino, e^+e^- , and γ temperature. The particle-antiparticle and spin-helicity statistical factors are $g_\nu = 2$, $g_{e^\pm} = 4$, $g_\gamma = 2$.

As computed in Ref.[9], not all products of e^+e^- -annihilation go into the photon gas, some go into overpopulating the neutrino distribution. We model this by an $\Upsilon > 1$ and assume that the neutrino temperature is not reheated. After e^+e^- -annihilation, the entropy in the corresponding volume is the sum of relativistic neutrinos with $\Upsilon > 1$ and photons

$$S_2 = \left(3S_\nu + \frac{2\pi^2}{45} g_\gamma T_{\gamma,2}^3 \right) V_2, \quad (28)$$

$$S_\nu = -\frac{g_\nu}{2\pi^2} T_{\nu,2}^3 \int_0^\infty H(u^2) u^2 du \quad (29)$$

where H is given by Eq.(22). Note that we must now distinguish between the neutrino and photon temperatures. The assumption that the neutrino temperature is not reheated implies that

$$T_1/T_{\nu,2} = a_2/a_1 = (V_2/V_1)^{1/3}. \quad (30)$$

Equating the two entropies and using this fact we obtain

$$\begin{aligned} \frac{T_{\gamma,2}}{T_{\nu,2}} &= \left(\frac{11}{4} + R \right)^{1/3}, \\ R &= \frac{21}{8} + \frac{135}{4\pi^4} \int_0^\infty H(u^2) u^2 du. \end{aligned} \quad (31)$$

Writing $\Upsilon = e^\sigma$ and expanding this to first order about $\sigma = 0$ gives

$$\left(\frac{4}{11} \right)^{1/3} \frac{T_{\gamma,2}}{T_{\nu,2}} = 1 - \frac{405\zeta(3)}{22\pi^4} \sigma \quad (32)$$

where $\zeta(x)$ is the Riemann zeta function. However, Eq. (32) is only applicable for relatively small σ . Figure 1 shows the ratio Eq. (31) as a function of Υ as obtained numerically, where we have ignored terms involving $m_\nu/T_f \simeq 10^{-6} \ll 1$. Note that for $\Upsilon = 1$, we obtain the usual value $T_{\gamma,2}/T_{\nu,2} = (11/4)^{1/3}$. Equal photon and neutrino temperature is obtained from $\Upsilon = 2.11$. The maximum value of Υ , for which all entropy goes into neutrinos, is approximately $\Upsilon = 2.91$.

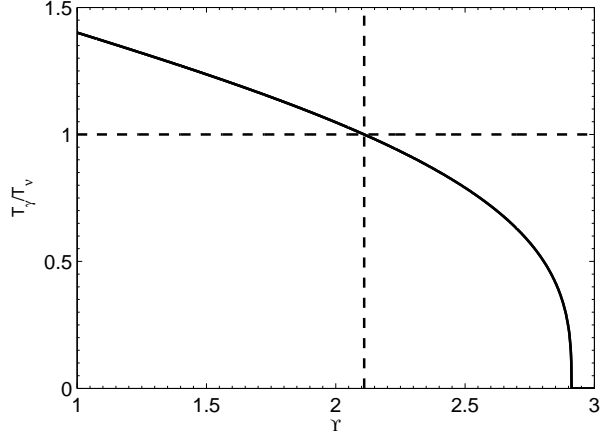


FIG. 1: Ratio of photon to neutrino temperature after reheating as a function of Υ .

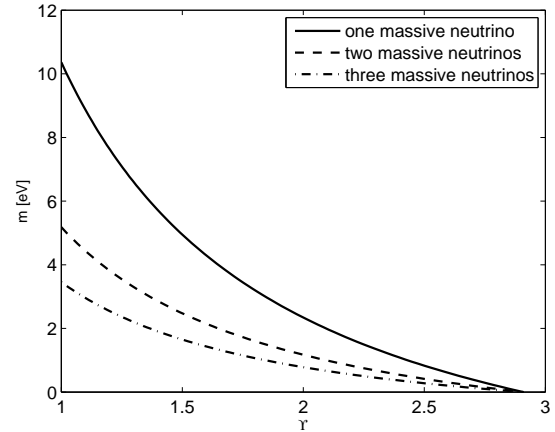


FIG. 2: Maximum neutrino mass as a function of Υ , obtained by equating neutrino and dark matter densities.

Using the measured CMB temperature and the above photon reheating calculation we obtain the current neutrino background temperature as a function of Υ . In turn, this allows us to set a bound on the mass of the heaviest neutrino(s) as a function of Υ by equating the neutrino energy density, Eq. (23), to the measured dark matter density, $\rho_{DM} = 8.934 \text{meV}^4$ [17]. We show the results in the case of one, two, or three equal mass neutrinos, where we set the mass of the lighter neutrino(s) to zero in Figure 2. The maximum allowed mass goes to zero in Figure 2 near to the maximum value of Υ from Figure 1 for a large range of values of ρ_{DM} . This is because for fixed T_γ , T_ν diverges to infinity as Υ approaches its maximum value, and hence the

neutrino energy density diverges to infinity as well. As we will see, we do not violate the dark matter limit in any of these three cases, since the value of Υ that is of most interest to us is near to $\Upsilon \simeq 1.1$, and the neutrino masses we consider are near to or below 1 eV.

III. EFFECTIVE NUMBER OF NEUTRINOS

A. Non-equilibrium model

Typically, when considering the evolution of the Universe the neutrino distribution is modeled as massless. The difference between the massless model and the more precise model based on the Vlasov equation that we derived above can be quantified as an effective number of neutrinos, defined by comparing the total energy density or pressure to a gas of massless particles and antiparticles

$$\sum_i \rho_i \equiv \frac{7}{120} \pi^2 N_{\nu, \rho}(T_\gamma, \Upsilon) \left(\frac{4}{11} \right)^{4/3} T_\gamma^4, \quad (33)$$

$$\sum_i P_i \equiv \frac{7}{360} \pi^2 N_{\nu, P}(T_\gamma, \Upsilon) \left(\frac{4}{11} \right)^{4/3} T_\gamma^4, \quad (34)$$

where the sum is over the three neutrino flavors and $(4/11)^{1/3}$ is the reheating factor when $\Upsilon = 1$, as is normally assumed. There are two different versions, depending on whether we define N_ν via pressure or energy density. The value given in [9] is defined using the neutrino energy density, and so we will do the same. From here on, N_ν will refer to $N_{\nu, \rho}$.

To compare the energy density Eq. (23) to that of a massless particle distribution, we make a change of variables $u = p/T_\nu$ and neglect terms involving $m/T_f \ll 1$

$$\rho^{EV} \simeq \frac{g_\nu T_\nu^4}{2\pi^2} \int_0^\infty \frac{(m^2/T_\nu^2 + u^2)^{1/2} u^2}{\Upsilon^{-1} \exp(u) + 1} du, \quad (35)$$

where the upper index ‘EV’ reminds us that we have used Einstein-Vlasov free streaming solution for the neutrino distribution. For $m \ll T_\nu$ this approximates the energy density of the equilibrium distribution of a massless fermion, but when T_ν is on the order of the mass, the mass term becomes important and changes the effective number of neutrinos. This is in addition to the increase in effective number of neutrinos due to $\Upsilon \neq 1$.

To explore the small m/T_ν limit, let $\Upsilon = e^\sigma$ and $\alpha = m/T_\nu$. As an illustration of the qualitative

behavior, we Taylor expand Eq. (35). Note that the following expansions will not be valid to the required precision in the regime where we will need numerical results

$$\rho^{EV} = \frac{7}{120} \pi^2 T_\nu^4 \left[1 + \frac{120}{7\pi^4} \left(\frac{9}{2} \zeta(3) \sigma + \frac{\pi^2 \alpha^2}{24} + \frac{\pi^2 \sigma^2}{4} + \ln 2 \sigma^3 + \frac{\ln 2}{2} \alpha^2 \sigma \right) \right], \quad (36)$$

where $\zeta(3) = \sum_{k=1}^\infty 1/k^3 = 1.20206 \dots$. In this same approximation regime

$$\frac{N_\nu^{EV}}{N} = \left(\frac{11}{4} \right)^{4/3} \frac{T_\nu^4}{T_\gamma^4} \left[1 + \frac{40}{7\pi^4} \sum_i \left(\frac{9}{2} \zeta(3) \sigma + \frac{\pi^2 \alpha_i^2}{24} + \frac{\pi^2 \sigma^2}{4} + \ln 2 \sigma^3 + \frac{\ln 2}{2} \alpha_i^2 \sigma \right) \right], \quad (37)$$

where $N = 3$ is the number of neutrino flavors in the standard model and the sum is over the three neutrino species. From this expansion, we can see the claimed increase in N_ν as the temperature decreases. We now give a more explicit approximation that is useful in the region of parameter space that we are most interested in. The coefficients of the quantities involving only σ are taken from Eq. (37), as that expansion is valid for the values of σ of interest when $\alpha = 0$. This allows us to match the large T_γ asymptotic behavior with a high degree of accuracy. The remainder of the coefficients are obtained via a nonlinear least squares fit to N_ν^{EV}/N

$$\begin{aligned} \frac{N_\nu^{EV}}{N} = & 1 + 1.861\sigma + 2.298\sigma^2 + .0296 \frac{\bar{m}^2}{T_\gamma^2} \\ & + 2.493\sigma^3 + .0357\sigma \frac{\bar{m}^2}{T_\gamma^2} + 2.574\sigma^4 \\ & + .0618\sigma^2 \frac{\bar{m}^2}{T_\gamma^2} - 4.79 \cdot 10^{-4} \sum_i \frac{m_i^4}{T_\gamma^4}, \end{aligned} \quad (38)$$

where $\bar{m} = \sqrt{\sum_i m_i^2}$ is the neutrino mass radius. The fit is valid to within 3.6% relative error in the region $1 \leq \Upsilon \leq 1.2$, $0 \leq m_i/T_\gamma \leq 5$. The coefficients differ from those in Eq. (37) since we have focused on achieving a fit near $m/T_\gamma \simeq 1$ where the effect we are investigating is most pronounced. In addition in Eq. (38), we have converted from neutrino to photon temperature using Eq. (31) to facilitate comparison with measured values.

The effect of mass becomes important when the neutrino temperature approaches the mass of the heaviest neutrino. For illustrative purposes, a plot of N_ν/N for three massive neutrino of mass .35eV

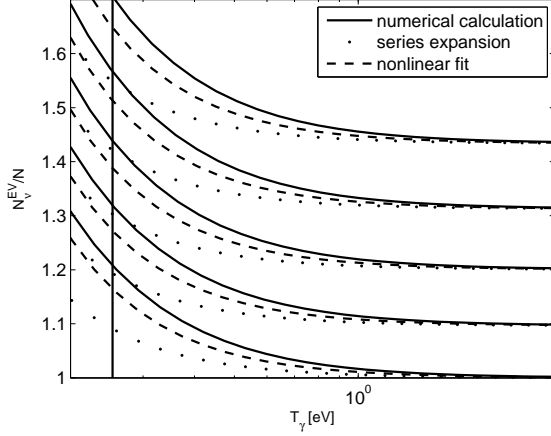


FIG. 3: Effective number of neutrinos derived from the energy density for three neutrinos of mass .35eV with fugacities Υ from 1 to 1.2 (solid lines bottom to top in increments of .05). The series expansions (dotted lines) and nonlinear fit (dashed lines) are also shown. The vertical line marks the photon temperature at recombination $T_r = .253\text{eV}$.

(solid lines) and various values of Υ is given in Figure 3. We also show the series expansion Eq. (37) (dots) and the nonlinear fit Eq. (38) (dashed lines). These graphs are approximately constant for $T_\gamma \gg T_r$, and so the values can be extrapolated back to BBN and are independent of the neutrino masses. From the high temperature expansion in Eq. (37) we see that to match $N_\nu = 3.71$ at BBN we require a fugacity of $\Upsilon = e^\sigma = 1.12$. If instead, the value computed in [9] is correct and the discrepancy is simply measurement error, we require a fugacity of $\Upsilon = 1.01$.

We can also expand the ratio of effective number of neutrinos at recombination to that at BBN, N_ν^r/N_ν^{BBN} , as a series in α and σ . To third order this equals

$$\frac{N_\nu^{r,EV}}{N_\nu^{BBN}} = 1 + \left(\frac{11}{4}\right)^{2/3} \frac{\bar{m}_\nu^2}{T_r^2} \left[\frac{5}{21\pi^2} - \left(\frac{14625}{539\pi^6} \zeta(3) - \frac{20}{7\pi^4} \ln 2 \right) \sigma \right], \quad (39)$$

where we have used Eq. (31) to replace the neutrino temperature with the photon temperature at recombination. We again perform a nonlinear least squares

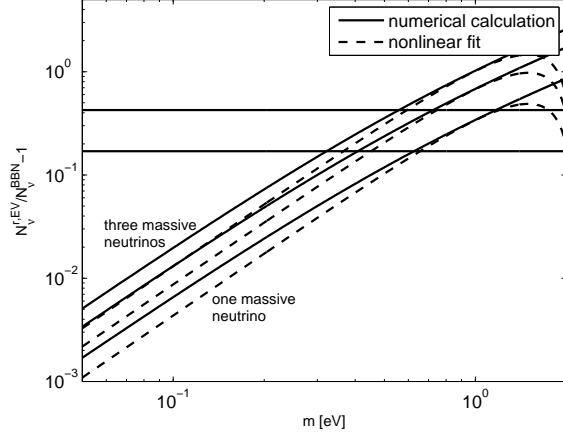


FIG. 4: Comparison of N_ν at recombination to N_ν at BBN for (bottom to top) one, two, and three massive neutrinos with fugacity $\Upsilon = 1.12$. The horizontal lines show the values corresponding to $N_\nu^{BBN} = 3.71$ (bottom line) and $N_\nu^{thBBN} = 3.046$ (top line).

fit for the coefficients

$$\frac{N_\nu^{r,EV}}{N_\nu^{BBN}} = 1 + .0281 \frac{\bar{m}^2}{T_\gamma^2} - .00122 \sigma \frac{\bar{m}^2}{T_\gamma^2} - 3.68 \cdot 10^{-4} \sigma^2 \frac{\bar{m}^2}{T_\gamma^2} - 3.99 \cdot 10^{-4} \sum_i \frac{m_i^4}{T_\gamma^4}. \quad (40)$$

The fit is valid to within 3.0% relative error in the region $1 \leq \Upsilon \leq 1.2$, $0 \leq m_i/T_\gamma \leq 5$. Figure 4 shows the variation of the ratio N_ν^r/N_ν^{BBN} as a function of the neutrino mass, in the cases of one, two, or three equal mass neutrino(s), setting the mass of the lighter neutrino(s) to zero. The result obtained by computing the ratio numerically using Eq. (31) and Eq. (33) is shown in solid lines and the nonlinear fit is shown in dashed lines. Note that at higher mass, we see the power law in \bar{m} start to break down as higher order terms in the expansion become important. The result is shown for $\Upsilon = 1.12$, but it is relatively insensitive to Υ . This can be seen from Eq. (39), since at lowest order there is no dependence on σ .

For the three possible cases of $N_M = 1, 2, 3$ (column 1 in table I), the values of the neutrino mass m_ν , which result in a rise of N_ν from $N_\nu^{thBBN} = 3.046$ (i.e. $\Upsilon = 1.01$) or $N_\nu^{BBN} = 3.71^{+0.47}_{-0.45}$ (i.e. $\Upsilon = 1.12^{+0.06}_{-0.07}$) to $N_\nu^r = 4.34^{+0.86}_{-0.88}$ are given in column 4. Depending on the data and analysis used, the neutrino mass values we find are close to, or outside of current cosmological bounds on the neutrino mass from WMAP data [18]. However, these bounds

TABLE I: N_M is the number of massive neutrinos assumed. The neutrino mass, m_ν is determined by connecting $N_\nu(T_{BBN})$ to $N_\nu(T_r)$. The last column shows the present day (PD) contribution of neutrinos to dark matter energy density, with Υ and the neutrino masses fixed to describe the increase of neutrino degrees of freedom from BBN to recombination epoch. Notation ${}^b c_a$ means that c is the central value bracketed by (a, b) .

N_M	$N_\nu(T_{BBN})$	$N_\nu(T_r)$	$m_\nu[\text{eV}]$	$\rho_\nu^{\text{PD}}/\rho_{\text{dark}}^{\text{PD}}$
1	3.046	$4.34^{+0.086}_{-0.88}$	$1.66^{1.13}_{0.528}$	$0.16^{0.11}_{0.05}$
2	3.046	$4.34^{+0.086}_{-0.88}$	$0.995^{0.703}_{0.347}$	$0.19^{0.14}_{0.07}$
3	3.046	$4.34^{+0.086}_{-0.88}$	$0.754^{0.542}_{0.275}$	$0.22^{0.16}_{0.08}$
1	$3.71^{+0.47}_{-0.45}$	$4.34^{+0.086}_{-0.88}$	$1.47^{0.627}_{0.0}$	$0.15^{0.072}_{2 \cdot 10^{-4}}$
2	$3.71^{+0.47}_{-0.45}$	$4.34^{+0.086}_{-0.88}$	$0.892^{0.408}_{0.0}$	$0.18^{0.092}_{10^{-4}}$
3	$3.71^{+0.47}_{-0.45}$	$4.34^{+0.086}_{-0.88}$	$0.680^{0.322}_{0.0}$	$0.21^{0.102}_{10^{-4}}$

could change based on the effect of neutrino mass and non-equilibrium distribution described here. A more robust bound for our purposes is the non-cosmological bound $m_\nu < 2.05\text{eV}$ [17] which we do satisfy.

We note that the scale of m_ν is non-negligible compared to the limit set in Figure 2, where we asked how large a mass is needed to describe all dark matter in the present day (PD) Universe. As a consequence, if the increase in N_ν central values were to be confirmed then the neutrinos emerge as a significant component in the dark matter inventory, altering the presumed energy inventory in the Universe [19]. In the last column in table I we present the fractional contribution of neutrinos to the present day dark matter component for all cases. Note that dark matter is 22% of the present day (PD) energy density in the universe [17].

B. Problems with Equilibrium Distribution

Here we show that a naïve application of equilibrium thermodynamics will produce a reduction of N_ν and remark on other issues that arise in such an approach. If one assumes an equilibrium distribution of massless neutrinos, or more precisely, negligible neutrino mass as compared to the ambient temperature, then the neutrino energy density scales as T_γ^4 , and hence the effective number of neutrinos, as defined in Eq.(33), is constant in time. Now suppose we use the fact that neutrinos are massive, but neglect the non-equilibrium FDEV aspects in the momentum distribution of particles. To make

this mistake, consider the energy density of each neutrino flavor to be, instead of Eq. (35),

$$\rho^{\text{eq}} = \frac{g_\nu T_\nu^4}{2\pi^2} \int_0^\infty \frac{(\alpha^2 + u^2)^{1/2} u^2 du}{\Upsilon^{-1} \exp(\sqrt{\alpha^2 + u^2}) + 1}. \quad (41)$$

Expanding this about $\alpha = 0 = m$ and $\sigma = \ln \Upsilon = 0$ to third order gives

$$\rho^{\text{eq}} = \frac{7}{120} \pi^2 T_\nu^4 \left[1 + \frac{120}{7\pi^4} \left(\frac{9}{2} \zeta(3) \sigma - \frac{\pi^2 \alpha^2}{24} + \frac{\pi^2 \sigma^2}{4} + \ln 2 \sigma^3 - \frac{\ln 2}{2} \alpha^2 \sigma \right) \right], \quad (42)$$

and hence

$$\frac{N_\nu^{\text{eq}}}{N} = \left(\frac{11}{4} \right)^{4/3} \frac{T_\nu^4}{T_\gamma^4} \left[1 + \sum_i \frac{40}{7\pi^4} \left(\frac{9}{2} \zeta(3) \sigma - \frac{\pi^2 \alpha_i^2}{24} + \frac{\pi^2 \sigma^2}{4} + \ln 2 \sigma^3 - \frac{\ln 2}{2} \alpha_i^2 \sigma \right) \right]. \quad (43)$$

Comparing this with the expression derived from the non-equilibrium distribution, Eq.(37), we find the opposite qualitative behavior in α .

Thus basing the analysis on a naïve equilibrium distribution, one would predict that N_ν decreases with temperature rather than increases. Hence one arrives at the incorrect qualitative behavior of N_ν unless both the neutrino mass and the non-equilibrium form of the neutrino distribution are accounted for.

The reader should note that there are other immediate problems with an equilibrium approach. The FD distribution does not conserve with diminishing temperature the comoving entropy and particle number content when $m \neq 0$. Even if we manipulated the value of Υ to preserve the particle number, we cannot also preserve the neutrino entropy since it is the nature of thermal equilibrium that entropy is exchanged with the heat bath and we would need to manipulate T to be able to preserve entropy, but that is controlled by other forces. We conclude that use of FD equilibrium distribution has multiple inconsistencies and in its most naïve application leads one to predict a reduction of N_ν in an expanding Universe.

IV. DISCUSSION

After the freeze-out, neutrinos freely stream through the expanding universe and their distribution function ceases to be thermal. Using a solution

of the Einstein-Vlasov equation, we find that as the universe cools and the temperature approaches the mass of the heaviest neutrino, the effective number of neutrino degrees of freedom, N_ν , increases. Such an increase is favored by the measurements of N_ν at BBN and electron-ion recombination. We have shown that this increase is due to the interplay of the neutrino mass and the non-thermal form of the neutrino distribution after freeze-out. Both these properties are essential for reaching the correct conclusion, i.e. that there is an increase in the effective number of neutrino degrees of freedom.

It is helpful to understand the essential physics of this observation without the need for much theory. In order to move from the number density, Eq. (25), to the energy density, Eq. (23), we weight the energy of a neutrino $E_\nu = \sqrt{p^2 + m^2}$ by the non-equilibrium free streaming FDEV distribution Eq. (8). The distribution preserves both the comoving particle number and entropy and, in case of neutrinos, the mass term in the distribution can always be neglected. However, one cannot neglect the mass in the energy of a neutrino E_ν , as at some point the momentum of a neutrino in an expanding universe will be small. Thus one weights a massive particle energy with an effectively massless distribution function at a temperature T_ν . It is possible to arrive at this result with entirely intuitive reasoning, the exact theoretical derivation is the essence of this report.

The values of m_ν seen in table I are close to or exceed various cosmological bounds [18]. However, these bounds could change when our non-equilibrium FDEV form Eq. (8) of the free-streaming neutrino distribution is incorporated in the analysis. Recall that there is no direct laboratory measurement of the magnitude of the neutrino mass except for the limit on electron-neutrino $m_\nu < 2$ eV derived from Tritium decay [17] which we satisfy. The differences between neutrino masses (squared) have been derived from observations of neutrino mixing, i.e. $\Delta m_{12}^2 = 75 \pm 2$ meV², $\Delta m_{23}^2 = 2320_{-80}^{+120}$ meV² [17]. Therefore some increase in N_ν between BBN and recombination is unavoidable.

Due to the large uncertainties in the measured N_ν values, they are still (barely) consistent with a scenario with three neutrinos whose mass is negligible, relative to the recombination temperature ($m_\nu \ll T_r$), and therefore results in a negligible increase in N_ν . Even so, note that to be consistent with the given error bounds, this requires $3.46 \leq N_\nu^{BBN} \leq 4.18$ which is larger than the calculated value and corresponds to $1.08 \leq \Upsilon \leq 1.19$. Thus, an important observation is that if one wants to main-

tain the calculated value $N_\nu^{thBBN} \simeq 3.046$ [9], then a neutrino mass on the order of the recombination temperature is required to account for the increased value N_ν^r .

To satisfy the often cited cosmological limit $\sum m_\nu < 0.6$ eV (this could be subject to change considering our results), and considering the lightest central value in table I ($m_\nu = 0.331$ eV), we see that all three neutrinos would need to be around $m_\nu \simeq 0.2$ eV in mass (i.e. $m_\nu^2 = 40,000$ meV²) in order to easily satisfy the measured values Δm^2 . For the case of three neutrinos of mass .2eV, we predict $N_\nu^r/N_\nu^{BBN} \simeq 1.07$. This is consistent with the measured range $0.83 \leq N_\nu^r/N_\nu^{BBN} \leq 1.60$. In general, we conclude that an increase in N_ν signals that the mass of the heaviest neutrino is near the recombination temperature T_r .

To conclude: We have shown that the observed increase in effective number of neutrinos as the temperature decreases is a natural consequence of the presence of non-equilibrium, free streaming FDEV neutrino distribution Eq. (8) after freeze-out. The deviation of the energy density of the FDEV non-equilibrium distribution from that of a Fermi-Dirac equilibrium distribution is due to the finite mass of the neutrinos. Within the standard model, the increase in effective number of neutrinos N_ν over time leading to the recombination epoch depends solely on the neutrino mass and presence of non-equilibrium distribution.

In table I we have presented explicit values for m_ν favored by the current knowledge of the values of N_ν . Note that the smaller the number of dominant mass neutrinos and the larger the change in N_ν needed between BBN and recombination, the larger is the value of m_ν we find. If little change in N_ν is needed, $m_\nu/T_r \rightarrow 0$. However, within the current error bounds, it is not possible to have negligible neutrino masses ($m_\nu \ll T_r$) when using the calculated value of N_ν^{thBBN} [9], see the first three lines in table I, where each entry has a lower finite m_ν . If the central values of $N_\nu(T_r)$ prevail within error bars, and no new mechanism is discovered to further increase $N_\nu(T_{BBN})$ then the relic neutrinos will have a mass above 0.275 eV and will contribute between 5% and 22% of the dark matter inventory in the Universe, or if relic neutrinos are counted as visible matter, they will increase the visible matter inventory noticeably, with the potential to double it.

Acknowledgments

This work has been supported by a grant from the U.S. Department of Energy, DE-FG02-

04ER41318 and by the Department of Defense (DoD) through the National Defense Science & Engineering Graduate Fellowship (NDSEG) Program.

-
- [1] A. Ringwald, “Prospects for the direct detection of the cosmic neutrino background,” Nucl. Phys. A **827**, 501C (2009) [arXiv:0901.1529 [astro-ph]]; and “How to detect the cosmic neutrino background?,” hep-ph/0301157.
 - [2] G. Tupper, B. Muller, J. Rafelski, and M. Danos, “On the detection of cosmic background neutrinos by acoustic phonon scattering,” Phys. Rev. D **35**, 394 (1987).
 - [3] A. D. Dolgov, “Neutrinos in cosmology,” Phys. Rept. **370**, 333 (2002) [hep-ph/0202122].
 - [4] J. Lesgourgues, and S. Pastor, “Massive neutrinos and cosmology,” Phys. Rept. **429**, 307 (2006) [astro-ph/0603494].
 - [5] S. Seager, D. D. Sasselov, and D. Scott, “How exactly did the universe become neutral?,” Astrophys. J. Suppl. **128**, 407 (2000) [astro-ph/9912182]; and “A new calculation of the recombination epoch,” Astrophys. J. **523**, L1 (1999) [astro-ph/9909275].
 - [6] S. Galli, R. Bean, A. Melchiorri, and J. Silk, “Delayed Recombination and Cosmic Parameters,” Phys. Rev. D **78**, 063532 (2008) [arXiv:0807.1420 [astro-ph]].
 - [7] C.-T. Yang, P. Chen J. Birrell, and J. Rafelski, Forthcoming.
 - [8] S. Hannestad, “Neutrino physics from precision cosmology,” Prog. Part. Nucl. Phys. **65**, 185 (2010) [arXiv:1007.0658 [hep-ph]].
 - [9] G. Mangano, G. Miele, S. Pastor, T. Pinto, O. Pisanti, and P. D. Serpico, “Relic neutrino decoupling including flavor oscillations,” Nucl. Phys. B **729**, 221 (2005) [hep-ph/0506164].
 - [10] P. D. Serpico, S. Esposito, F. Iocco, G. Mangano, G. Miele, and O. Pisanti, “Nuclear reaction network for primordial nucleosynthesis: A Detailed analysis of rates, uncertainties and light nuclei yields,” JCAP **0412**, 010 (2004) [astro-ph/0408076].
 - [11] E. Komatsu *et al.* [WMAP Collaboration], “Seven-Year Wilkinson Microwave Anisotropy Probe (WMAP) Observations: Cosmological Interpretation,” Astrophys. J. Suppl. **192**, 18 (2011) [arXiv:1001.4538 [astro-ph.CO]].
 - [12] G. Steigman, “Neutrinos and Big Bang Nucleosynthesis,” arXiv:1208.0032 [hep-ph].
 - [13] H. Andreasson, “The Einstein-Vlasov System/Kinetic Theory,” Living Rev. Rel. **14**, 4 (2011) [arXiv:1106.1367 [gr-qc]].
 - [14] C. Cercignani, and G. Kremer. *The Relativistic Boltzmann Equation: Theory and Applications*. Birkhuser Verlag, Basel, 2000.
 - [15] Y. Choquet-Bruhat. *General Relativity and the Einstein Equations*. Oxford University Press, Oxford, 2009.
 - [16] J. Ehlers. “Survey of general relativity theory” In *Relativity, Astrophysics and Cosmology*, **38**, pp 1–125, D. Reidel Publishing Company, Dordrecht-Holland, 1973.
 - [17] J. Beringer *et al.* [Particle Data Group Collaboration], “Review of Particle Physics (RPP),” Phys. Rev. D **86**, 010001 (2012).
 - [18] A. Goobar, S. Hannestad, E. Mortsell and H. Tu, “A new bound on the neutrino mass from the sdss baryon acoustic peak,” JCAP **0606** (2006) 019 [astro-ph/0602155].
 - [19] M. Fukugita, and P. J. E. Peebles, “The Cosmic energy inventory,” Astrophys. J. **616**, 643 (2004) [astro-ph/0406095].